Chapter 9

A rainfall–runoff scheme for use in the Hamburg climate model

L. DÜMENIL and E. TODINI

Abstract

With a view to increasing the realism of the description of land surface processes in the Hamburg climate model, a scheme is introduced that accounts for the partition of rainfall at the ground between infiltration into the soil and surface runoff. The scheme was adapted and calibrated for the catchment of the river Arno and takes the heterogeneity of the land surface within a grid area into account. For the use in the general circulation model it has been expanded to account for stronger runoff components in regions of mountainous terrain. The GCM simulated annual globally averaged runoff is found to be in good agreement with observations.

1. Introduction

Many scientific institutions worldwide are involved in studying global climate and global change. The general public also is becoming increasingly aware of these issues. Any scientific statement concerning these problems must be founded on sound scientific grounds, and must take into account state-of-the-art knowledge on all the important processes of the climate system. In this field, experimentation can only be carried out with the help of powerful coupled models of the general circulation of the atmosphere and oceans (OAGCMs). Until recently only relatively low horizontal and vertical resolution could be afforded in climate modelling. Apart from this problem, the areas which require research in the atmospheric part of these models are i.a. the representation of clouds and the various components of the hydrological cycle. In particular, the hydrological processes at the land surface, have so far only been represented in OAGCMs in a rather rudimentary way.

As an initial step to expand the level of complexity of land surface processes in the Hamburg OAGCM (Fischer, 1987), we shall introduce a scheme that accounts for the partition of rainfall between infiltration into the soil and surface runoff. The so-called Arno (or Xinan-Jiang) scheme was derived from catchment considerations and takes the heterogeneity of the land surface within a grid area into account. It is designed to compute, for a given rainfall event, (a) the amount of water at the surface that will infiltrate into the soil in the regions where the soil is not yet saturated, and (b) the amount of water that will run off in the regions where the soil has reached saturation.

2. Runoff in the context of general circulation models

2.1. *Motivation*

When the new second generation Hamburg model ECHAM was developed, the need for improvement of this particular aspect of the model was identified. This was motivated by two facts. The first is due to the task of coupling atmosphere and ocean models. Because of the presence of the ocean, several processes need to be considered in the coupled atmosphere–ocean system that are traditionally neglected in weather forecasting models.

In contrast to weather forecasting models, sea-ice cover is required as a prognostic variable, as is the freshwater flux. The latter is a variable that influences both the thermohaline circulation in the ocean and the formation of sea-ice via its influence on salinity. It is therefore a critical variable for the evolution of climate. Over the oceans, the freshwater flux is normally taken as $P - E$, precipitation minus evaporation. Over land the process is more complex. The water reaching the surface during precipitation events is distributed locally between infiltration into the soil and immediate runoff at the surface. The water is then transferred to the rivers and eventually to the sea. Depending on the local soil and orographic as well as other conditions, drainage from the wet soils may also add to the river flow, and some water percolates from the soil to the water table underneath.

The first generation of the Hamburg climate model (Fischer, 1987) consisted of a low-resolution version of the European Centre for Medium Range Weather Forecasts' (ECMWF) weather prediction model. Due to their specific task and their relatively short integration times of not more than 10 days, the results of weather prediction models are influenced by land surface processes to a lesser degree than climate models which are typically integrated for decades. Land surface processes are therefore only computed in a rather rudimentary way. In this model, the time evolution equation of soil water was updated according to the scheme of Deardorff (1972). This scheme is not acceptable for climate studies because it relies on an updating process based on present-day climatology and does not take hydrological information into account. The amount of water that goes into runoff is normally not of interest in a ten-day forecast.

The Deardorff scheme assumes the same type of force-restore method for water in the soil as for heat conduction. Evaporation loss and input due to precipitation events are components of the soil water budget. The full equations are approximated by two prognostic equations for two layers of soil water and allow a diffusive exchange between these layers. A value specified from climatology (Mintz and Serafini, 1981) is used as the lower boundary condition. If the prescribed soil field capacity for either layer is reached, runoff may occur. This gives the old scheme the character of the "bucket scheme" that was implemented e.g. in the GFDL OAGCM by Manabe (1969). For climate research in particular, the aspect of a fixed climate boundary condition at all times is unacceptable.

While the processes associated with soil hydrology are relatively well understood and may be modelled successfully and in great detail at the point, element and small catchment scale, they cannot yet be modelled at the same level of detail at the scale of very large river catchments (continental scale). OAGCMs on the other hand will still be limited, for a considerable length of time, to relatively large grid sizes, since their application, in the context of climate change, requires typical integration times of the order of 100 years. Although the resolution may well improve over the next decade, enabling us to resolve at least medium-sized river catchments, a process of up-scaling of our knowledge of hydrologic processes will still have to be initiated in order to incorporate these processes in OAGCMs at sufficient detail for global climate forecasts.

In the meantime, relatively simple but physically based approaches have to fill this gap in the representation of the hydrological cycle. It is required that they can take the heterogeneity of the land surface within a grid area into account.

The motivation to replace the Deardorff scheme was therefore two-fold: In the climate model, all processes have to be formulated such that they are independent of present-day climatology, because this would otherwise preclude the simulation of e.g. paleo-climates. Second, the concept of the Deardorff scheme may well be appropriate for heat diffusion and in medium-range forecasts, but it is not based on the knowledge of hydrological processes and their time-scales. In order to incorporate more hydrology into their parameterisation scheme, an approach different from the simple "bucket" model was adopted in the UK Meteorological Office model (Warrilow et al., 1986). Here, the Richards' equation is simplified and applied at each grid-cell. For us, this approach did not seem to be a good alternative, one reason being the fact that this type of equation is only valid at a single point. Specific, and so far undeveloped, techniques are required in order to extend this scheme beyond the microscale.

Although more sophisticated rainfall–runoff schemes are available in hydrological engineering applications [Stanford Watershed Model IV (Crawford and Linsley, 1966), National Weather Service Soil Water Accounting Model (Burnash et al., 1973), SSAR (Rocwood and Nelson, 1966), Continuous API (Sittner et al., 1969), TANK (Sugawara et al., 1976), SHE (Abbott et al., 1986)], their implementation in OAGCMs is strongly inhibited by the lack of data for verification and initialisation of such schemes on the global scale. Even though many applications in hydrology provide excellent data coverage at specific points, more data will be needed on the distributions of soil characteristics, the heterogeneity (and how it influences the mean over a grid area) of the land surface, the distribution of water with depth in the soil and the movement of the water table with the seasons. All of these are at present poorly understood, but field campaigns are being initiated in order to improve the required data base. For the time being, it is therefore recommended to keep the scheme as simple as possible and the number of tuning parameters at a minimum.

The catchment scheme to be introduced below is a simple extension of the "bucket" scheme, from the point of view of an atmosphere modeller, and a simplification of the more sophisticated hydrology schemes that are employed in water resources research and engineering. The scheme has been successfully applied to the catchment of the river Arno in Italy. Input and output and the basic assumptions are such that the model is independent of the present-day climate and should be equally applicable at all model resolutions (i.e. grid cells of 5.0° × 5.0° or 1.0° × 1.0°).

2.2. *The ECHAM Model*

As mentioned above, the atmospheric part of the Hamburg climate model has evolved in several steps. The ECMWF model was used initially (Fischer, 1987). It was replaced by the ECHAM model, where most of the original parameterisations for cloud cover, radiation, horizontal diffusion and heat flux in the soil and the water reservoir, were replaced by revised schemes. In particular the treatment of the boundary conditions over land was modified in order to provide a better physical basis for climate, i.e. long-term, integrations. The spectral formulation of the original model was, however, retained. A detailed description of this so-called ECHAM version of the model and its climatology is available in Roeckner et al. (1989, 1992).

All model results, which will be discussed later, are taken from the ECHAM model integrated at T21 resolution (equivalent to a grid spacing of 5.625° longitude, i.e. typical grid size of 600 km × 600 km). In the ECHAM model, the following land surface processes are represented. Precipitation may reach the ground as rain or snow. At the surface, a single reservoir for soil water evolves with time using infiltration and evaporation as input. The Arno scheme has been integrated interactively in the GCM to specify how much rainfall is available for runoff and infiltration, respectively. The model calculates evaporation from the atmospheric demand which is then modified by a simple vegetation scheme (Blondin, 1989) to give the actual evapotranspiration. This is subtracted from the soil water reservoir. In cold conditions precipitation may fall as snow and will accumulate on the ground. When this snow-pack begins to melt, the melt water goes directly into surface-runoff if the ground underneath is still frozen. If the ground is thawing, the snow melt water also enters the Arno scheme.

After the computation of infiltration, drainage and runoff at the grid cell, the water is subjected to a linear advection scheme (Sausen et al., 1991) which collects the runoff in large river catchments and transfers it to the oceans.

3. Description of the Arno scheme

Over a large catchment (or a grid cell), saturated and unsaturated regions are unevenly distributed. There may be areas in the vicinity of rivers and streams that are saturated most of the time, whereas slopes and areas with certain soil conditions never reach saturation at all. If it rains, the regions with small field capacities will produce runoff at once, whereas in regions where field capacities are relatively large, rain water arriving at the surface may infiltrate for a certain period of time, i.e. until the local soil field capacity is filled and saturation is reached. Only from then onwards, will further rainfall produce runoff. Soils that have reached soil water values close to saturation, experience a depletion of soil water by the processes of drainage and percolation to the water table. Runoff and drainage are collected and transported horizontally in catchments of various sizes and eventually take the precipitated water to the oceans where it enters as fresh water inflow.

Bucket schemes, as they have been used so far, operate on the assumption that the soil water available in a catchment area is evenly distributed over the whole area. This means that no runoff will occur in a catchment until the whole area reaches saturation. Usually bucket schemes do not account for drainage and percolation.

The scheme presented here tries to describe the process of infiltration and runoff (including drainage) based on simple hydrological experience. The main point is that, unlike the bucket model, it takes the heterogeneous distribution of soil water capacity into account.

3.1. *Derivation of the equations*

The basic foundation of the model is derived from the integration over the whole catchment of the equation of water balance at a point on the ground.

The original model was developed by R.J. Zhao at the East China Technical University of Water Resources at Nanking (now HeHai University), and is known as the Xinan-Jiang model (Zhao, 1977).

Subsequently, the original scheme was modified by Todini (1988) in order to take into account, more effectively, the effect of drainage on soil depletion. Drainage, together with evapotranspiration, is responsible for the highly non-linear behaviour of the catchment response.

The equation that expresses the local mass balance at one point in the basin is:

$$r = \begin{cases} p - (w - w_0) & \text{if } p > w - w_0 \\ 0 & \text{if } p \leq w - w_0 \end{cases} \tag{3.1}$$

where r is the local surface runoff (mm), p is the local precipitation (mm), w is the local storage capacity (mm), and w_0 is the initial uniform water content in the soil (mm) within the basin.

The total volume of runoff produced over the entire basin may be expressed by the average depth R, i.e. by the integral:

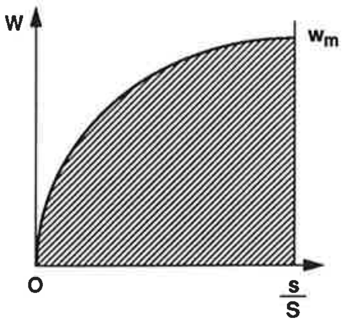

Fig. 1. Schematic of the distribution of soil water capacities at the point scale. The shape of the curve is determined by the parameter b and the total grid cell soil water content is W_m.

$$R = \frac{1}{S}\int_0^S r\,\mathrm{d}s = \frac{1}{S}\int_0^S [(p - (w - w_0)]\,\mathrm{d}s \tag{3.2}$$

where R is the mean integral value of the runoff, and S is the total area of the basin.

The total soil capacity of the catchment consists of the aggregate of many different local soil water capacities that depend on the type of soil. In other words, for a given catchment, the storage capacity is not represented by a unique value as is assumed in a bucket model, but by a set of values with a probability density distribution $f(w)$.

It is possible to define the "storage capacity distribution curve" as a curve which defines the percentage s/S of the basin area in which the storage capacity is less than or equal to an assigned value w. It is expressed as follows:

$$\frac{s}{S} = 1 - \left(1 - \frac{w}{w_m}\right)^b = F(w) = \int_0^w f(\xi)\,\mathrm{d}\xi \tag{3.3}$$

where w is the storage capacity value, $0 < w \leq w_m$; w_m the maximum soil water capacity in the basin; b the characteristic parameter of the basin; and $F(w)$ the cumulative probability function of the random variable w.

The shaded area between the curve and the x-axis in Figure 1 represents the average storage capacity of the entire basin, which is indicated by the symbol W_m as:

$$W_m = \int_0^1 w\,\mathrm{d}\left(\frac{s}{S}\right) = \frac{1}{S}\int_0^S w\,\mathrm{d}s \tag{3.4}$$

Figure 2 illustrates how the rainfall is distributed between runoff and infiltration. Let us assume that initially the soil water reservoir does not contain any water. Precipitation event 1 makes a certain amount of water available which is P_1. As we have no measure as yet on how the precipitation is distributed over the catchment area, we assume an even distribution, indicated by the straight horizontal line in Figure 2. The point where this line intersects the curve for w, separates the saturated and unsaturated parts of the catchment. Where P_1 exceeds w, runoff may occur, where $P_1 < w$, the water infiltrates into the ground. The total water content of the reservoir in the ground integrated over the catchment is now W_0.

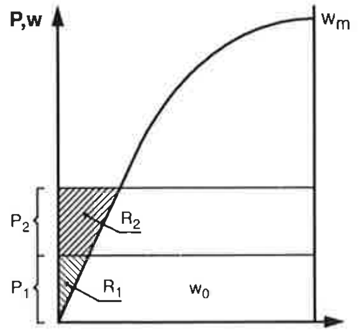

Fig. 2. Distribution of rainfall between runoff and infiltration for two precipitation events with the same amount of water. $P_{1,2}$ are evenly distributed over the grid cell, P_1 begins at zero initial water content, P_2 at initial water content W_0.

The next precipitation event P_2 starts from the condition of a partly filled reservoir. If we assume $P_2 = P_1$, the area of saturation where runoff may occur is now much larger and consequently a larger percentage of P_2 appears as runoff than was the case for P_1.

The calculation of runoff may then be expressed in the form:

$$R = P - (W_m - W_0) \tag{3.5a}$$

for:

$$P > (1 + b)W_m\left(1 - \frac{W_0}{W_m}\right)^{\frac{1}{b+1}}$$

or by:

$$R = P - (W_m - W_0) + W_m\left[\left(1 - \frac{W_0}{W_m}\right)^{\frac{1}{b+1}} - \left(\frac{P}{(b+1)W_m}\right)^{b+1}\right] \tag{3.5b}$$

for:

$$P \leq (1 + b)W_m\left(1 - \frac{W_0}{W_m}\right)^{\frac{1}{b+1}}$$

where the upper case quantities indicate integral mean values.

These equations of state must be associated with the balance equation by which the mean water content in the soil is updated.

The equation takes the form:

$$W_0(t + \mathrm{d}t) = W_0(t) + P(t) - E(t) - R(t) - D(t) - I(t) \tag{3.6}$$

where $E(t)$ is the loss through evapotranspiration between t and $t + \mathrm{d}t$, $D(t)$ is the

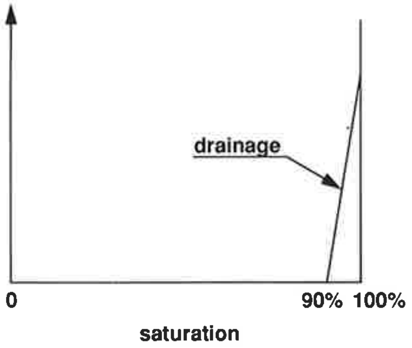

Fig. 3. Drainage of water in the soil adds to the local runoff. Drainage occurs as a linear function of total soil water in the range of 90–100% saturation.

loss through drainage between t and $t + \mathrm{d}t$, and $I(t)$ is the percolation loss to deep water tables between t and $t + \mathrm{d}t$.

The drainage term $D(t)$ is generally linked to the water content of the soil (Figure 3) in non-linear form and can be expressed as follows:

$$D(t) = \begin{cases} \alpha D_{\max}\dfrac{W_0}{W_m} & W_0 \le W_D \\ \alpha D_{\max}\dfrac{W_0}{W_m} + (1-\alpha)D_{\max}\left(\dfrac{W_0 - W_D}{W_m - W_D}\right)^c & W_0 > W_D \end{cases} \tag{3.7}$$

where α is the percentage of maximum drainage at maximum water content W_m; $D_{\max}$ the maximum drainage; W_D the water content threshold value; and c the exponent of the variation law: $c = 1$ linear, $c = 2$ quadratic. Upper case quantities indicate mean integral values.

The quantity $I(t)$ varies only slightly over time when compared to the other terms; nevertheless a non-linear behaviour may be assumed for this, which may be expressed as follows:

$$I(t) = \begin{cases} 0 & W_0 \le W_i \\ \beta(W_0 - W_i) & W_0 > W_i \end{cases} \tag{3.8}$$

where W_i represents the water content threshold value for calculating deep infiltration.

Finally, the term $E(t)$ may be derived from the evapotranspiration ET_0 reference value by means of suitable crop coefficients and taking into account the actual quantity of water present in the soil.

The total outflow $R_T(t)$ produced by the precipitation $P(t)$ is finally:

$$R_T(t) = R(t) + D(t) + B(t) \tag{3.9}$$

where $B(t)$ is the outflow originating from deep water tables.

3.2. Modifications for use in the OAGCM

As was shown in the previous section, the scheme can be reduced to a set of equations which only uses information on the average quantity of initial water content and current water content of the total soil reservoir. It is therefore a parameterisation in the true sense, because it expresses sub-grid scale variability and processes in terms of the averaged large-scale value. This is a familiar concept which is used for many physical processes that cannot be resolved explicitly in general circulation models.

The scheme also fulfils another requirement of OAGCMs because of its simplicity: the same set of calculations is executed at each land point in the OAGCM. This is an important pre-requisite for an efficient use of today's vector processing computers.

The scheme was originally designed with specific catchments in mind (Xinan-Jiang and Arno river; Todini, 1988). The equations are, however, general and simple enough to allow the application of the scheme to a grid cell in the general circulation model. There is also no general limitation to the size of the area to which the scheme may be applied.

A further advantage of the scheme is that it has a very small number of parameters which need to be specified. In a specific catchment the range of these parameters may be established from observational data to which the model is applied and which can be used for model calibration. Figure 4 shows part of the catchment of the Arno river in northern Italy to which the scheme was originally adapted for river-flow forecasting. The gauge data from this river was used to calibrate the model (Figure 5a). Calibrated in this way, the model produces a forecast which is in very good agreement with observed gauge data taken from another period (Figure 5b; Todini, 1988).

For application in the OAGCM we have adopted the following guidelines. In the OAGCM all land surfaces have at present the same thermal characteristics everywhere, if they are not covered by snow or ice. We have therefore assumed the same value of W_m for the maximum grid-cell soil-water saturation-capacity at all OAGCM land points.

In a catchment, a typical average value for the parameter b would be $b = 0.2$. We chose to modify this parameter at grid cells with steep orography. In this way, the scheme is expected to produce more than average runoff in mountainous regions. This orography correction to b is made dependent on the model resolution:

$$b = \max\left[\frac{\sigma_h - \sigma_0}{\sigma_h + \sigma_{\max}} : 0.01\right] \tag{3.11}$$

Values of b lie within the range 0.01 to 0.5, when the minimum and maximum standard deviations of orography, σ_0 and $\sigma_{\max}$, are used, namely:

$$\sigma_0 = 100\ \mathrm{m} \tag{3.12}$$

$$\sigma_{\max} = 1500\ \mathrm{m\ at\ T21}, \quad \text{or } \sigma_{\max} = 1000\ \mathrm{m\ at\ T42\ resolution}$$

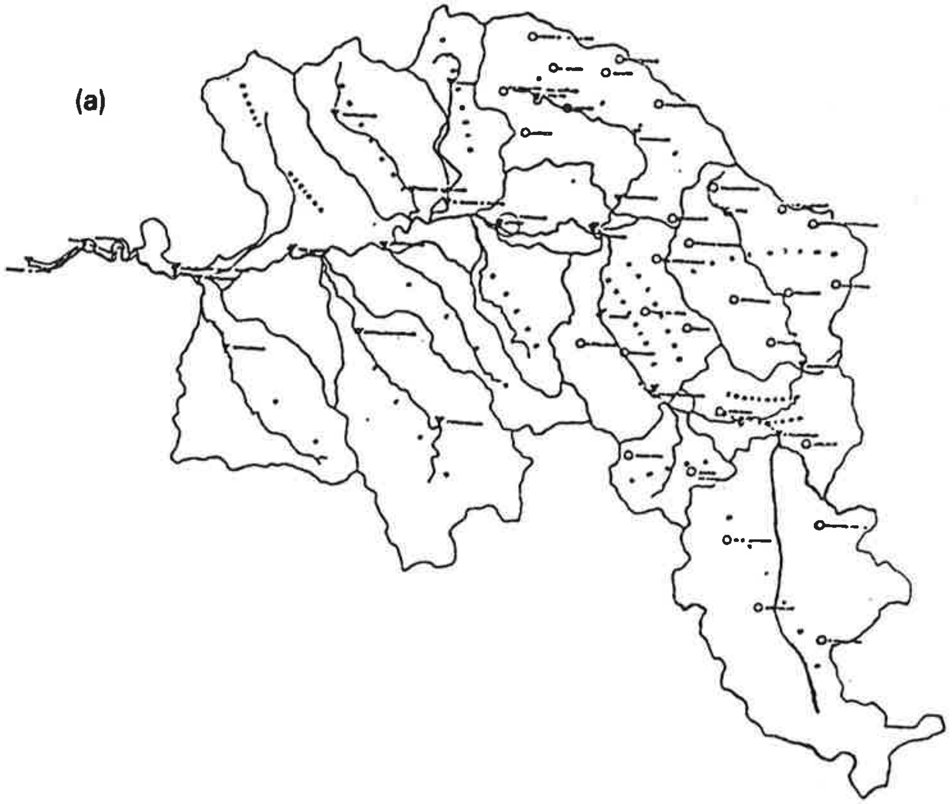

Fig. 4. a. The catchment of the Arno river in northern Italy and the hydrological gauge network.

Furthermore, the scheme is extended to OAGCM areas covered with snow or ice. From the equation for the OAGCM snow pack on the ground, we can deduce the amount of water that becomes available during the melting of the snow. If the soil underneath the snow pack is frozen, all melt water goes directly to runoff. If the soil is not frozen, the melt water is subjected to the runoff/infiltration scheme as described in section 3.1.

The drainage component of the runoff at a grid cell R_D is computed from equation (3.7) if the soil has reached more than 90% of its field capacity and if the soil is not frozen:

$$R_D = \begin{cases} d_{\min}\dfrac{W_s}{w_{\max}} & \text{if } W_s < W_{DR} \\[2ex] d_{\min}\dfrac{W_s}{w_{\max}} + (d_{\max} - d_{\min})\left(\dfrac{W_s - W_{DR}}{W_{\max} - W_{DR}}\right)^D & \text{if } W_s \geq W_{DR} \end{cases} \qquad (3.13)$$

with $d_{\min} = 0.0005$ mm/hr, $d_{\max} = 0.05$ mm/hr, $W_{DR} = 0.90 W_{\max}$ and $D = 1.5$.

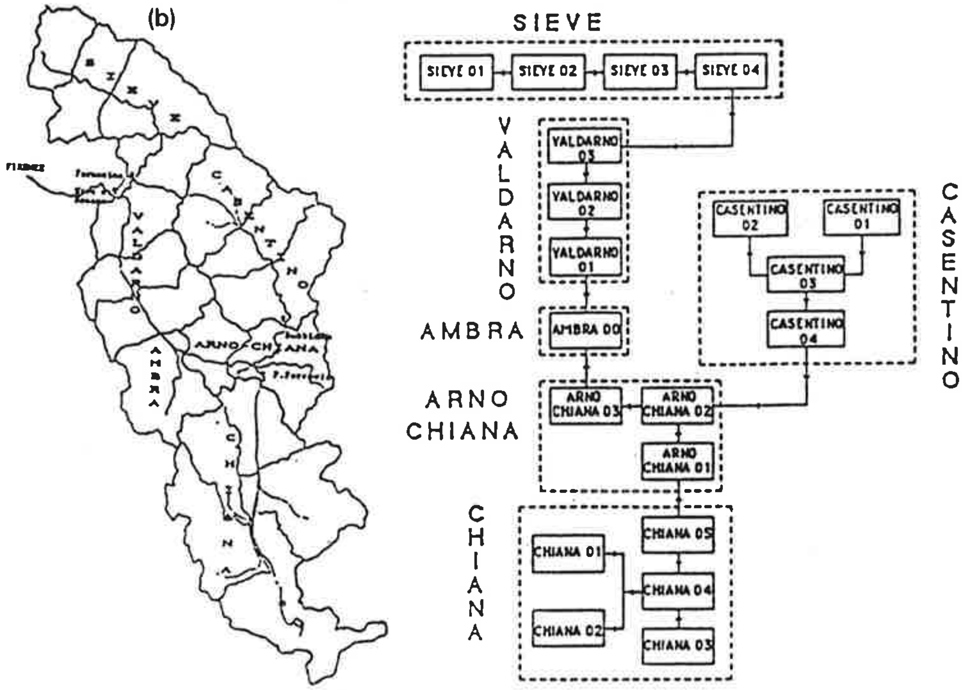

Fig. 4 (continued). b. Schematic of the sub-catchments used in flood forecasting with the Arno model.

The percolation component, I, that is contained in the catchment version of the scheme is neglected in the present version of the scheme, because no extra information on the water table is available in the model.

4. The simulated hydrological cycle

The model parameters and processes associated with the hydrological cycle are an important part of any OAGCM simulation. Due to the lack and insufficiency of climatological data for these fields on the global scale, the model generated fields are, however, difficult to validate in detail. In the following, we shall qualitatively assess the precipitation field, the surface runoff generated by the Arno scheme, the soil water reservoir, and the output from the river runoff scheme during the seasonal cycle. In this first attempt to verify model results, we shall try mainly to establish the plausibility and consistency of the simulated fields which are all inter-related.

All results are monthly means taken from a 20-year integration using the ECHAM2-T21 model as described in section 2. In the simulation, diurnal and seasonal cycles of solar insolation are applied.

A first crude comparison of the parameters of the hydrological cycle with climatology is given in Figure 6 (Roeckner et al, 1992). Evaporation, precipitation

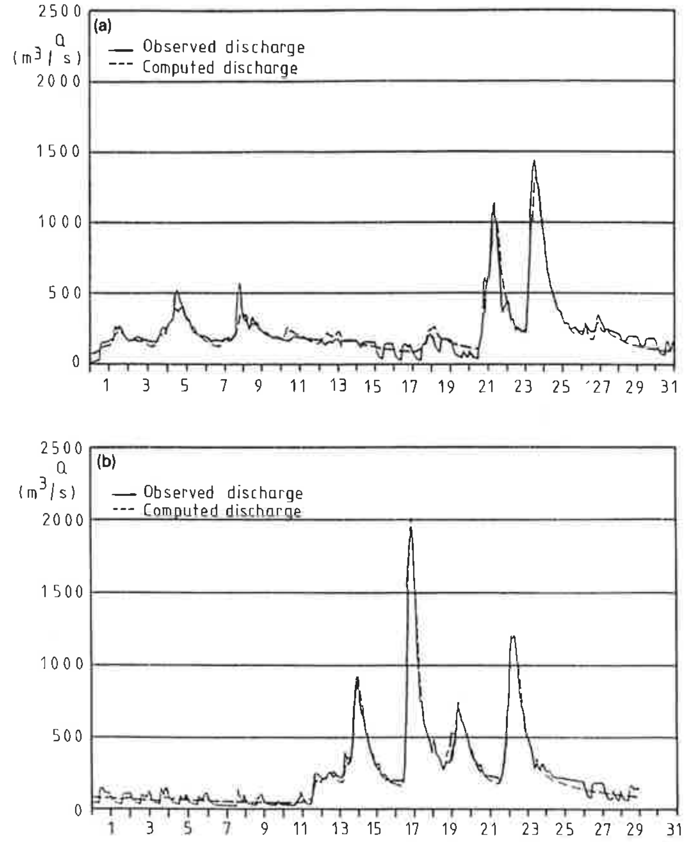

Fig. 5. Application of the Arno scheme to hydrological data. (a) Calibration of the model using data from December 1959. (b) Hind-casting of the flooding in February 1960: model results and verification data.

and runoff are compared to observations by Baumgartner and Reichel (1975). The globally averaged long-term annual mean values of the hydrological parameters simulated over land are in good agreement with the climatology, but are smaller than observed. Compared to the climatology, there is less precipitation arriving at the continental surface and less evaporation. Although the amount of freshwater that is made available to the oceans by the continental runoff is close to the observed, a relatively large amount of precipitation is taken out of the cycle and stored in the permanent snow packs on the continents such as Greenland and Antarctica. The model does not account for the freshwater input into the ocean that occurs directly from glaciers by the process of calving.

4.1. Precipitation

Figure 7 displays the model simulated field of total precipitation for January and July. Model results are compared to the climatology by Jaeger (1976) and

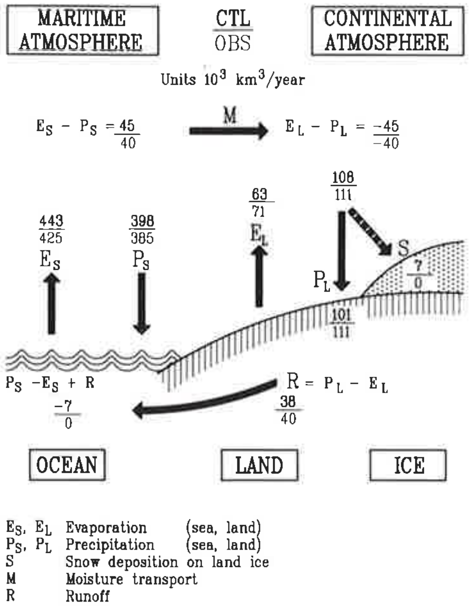

Fig. 6. Global annually averaged hydrological cycle from a 20-year model simulation (ECHAM2, upper values), and the climatology by Baumgartner and Reichel (1975; lower values).

a more recent one by Legates (1987) and Legates and Willmott (1989). A good representation of the global field of precipitation by the model's dynamics and convection parameterisation schemes is, of course, the pre-requisite for a successful simulation of the runoff process. The precipitation field simulated by the ECHAM2-T21 model compares favourably with the Jaeger climatology and with results from other models of the same resolution, but lacks many details. (The structure of this field is smoothed due to Jaeger's data sampling at 5° intervals which is about the same resolution as that of the present model.)

In general, the model has a tendency to broaden precipitation events of convective or orographic origin so that some of the maxima that are present in the climatology are not simulated. In January, e.g., there is no maximum at the southernmost tip of South America, and in Africa, the ITCZ is not well pronounced so that the dry regions extend almost to the equator. In South America the model produces much less rainfall than is observed due to systematic model errors which also occur in other low resolution models. Where precipitation is dominated by large-scale processes, e.g. in the Northern Hemisphere storm tracks, the precipitation either as rain or snow is steered by the cyclone paths. In Europe in winter, cyclones penetrate into the continent in a realistic way and a much better snow pack is simulated than in North America (Behr and Dümenil, 1991). In particular the behaviour of cyclone tracks in North America in the spring is affected by systematic model errors so that the precipitation in the middle of the continent is overestimated.

(a)

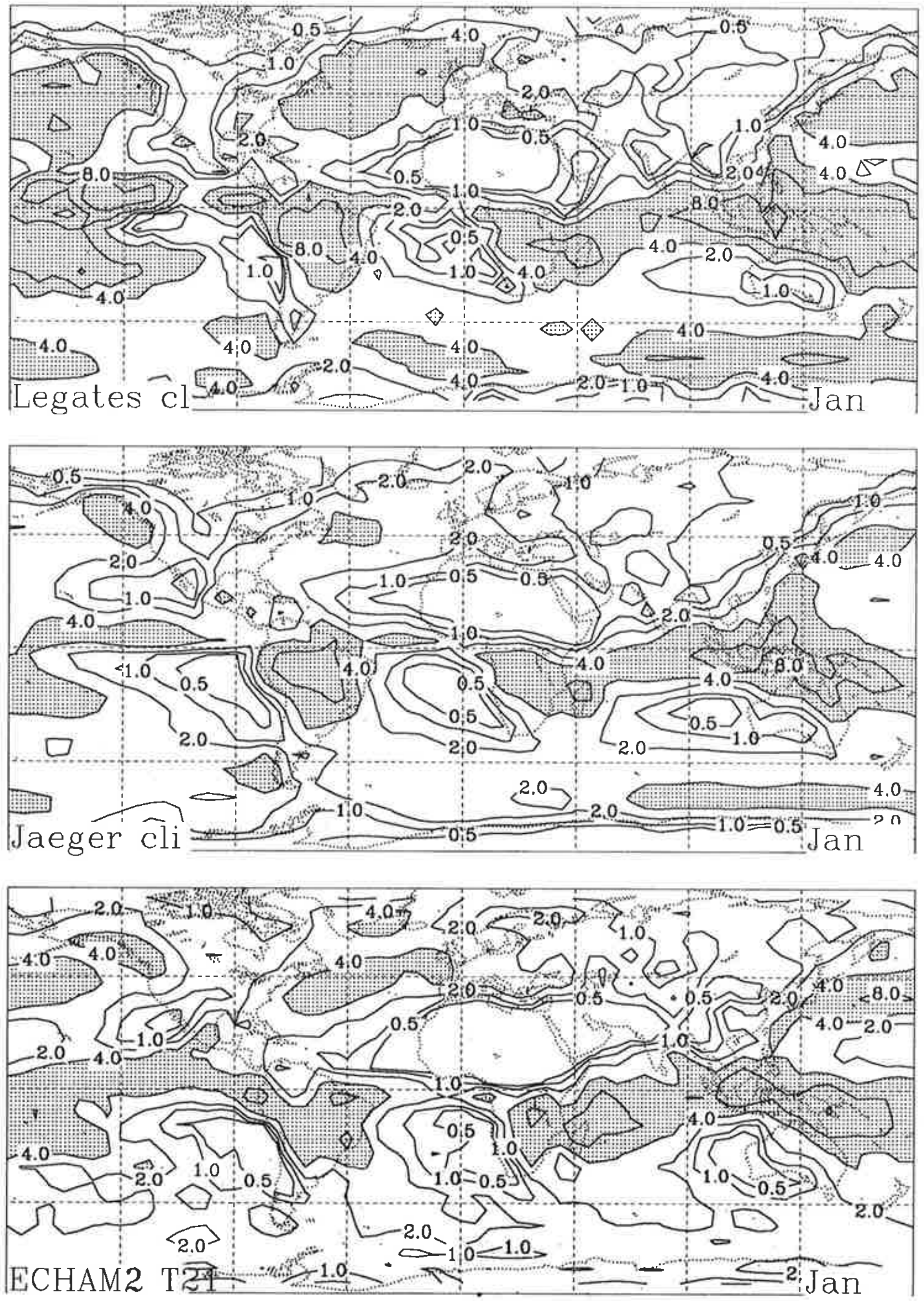

Fig. 7. a. Horizontal distribution of total precipitation for the month of January. Climatologies by Legates (1987) and Legates and Willmot (1989; top), Jaeger (1976; middle) compared to monthly mean values from a 20-year integration with the ECHAM model (bottom).

(b)

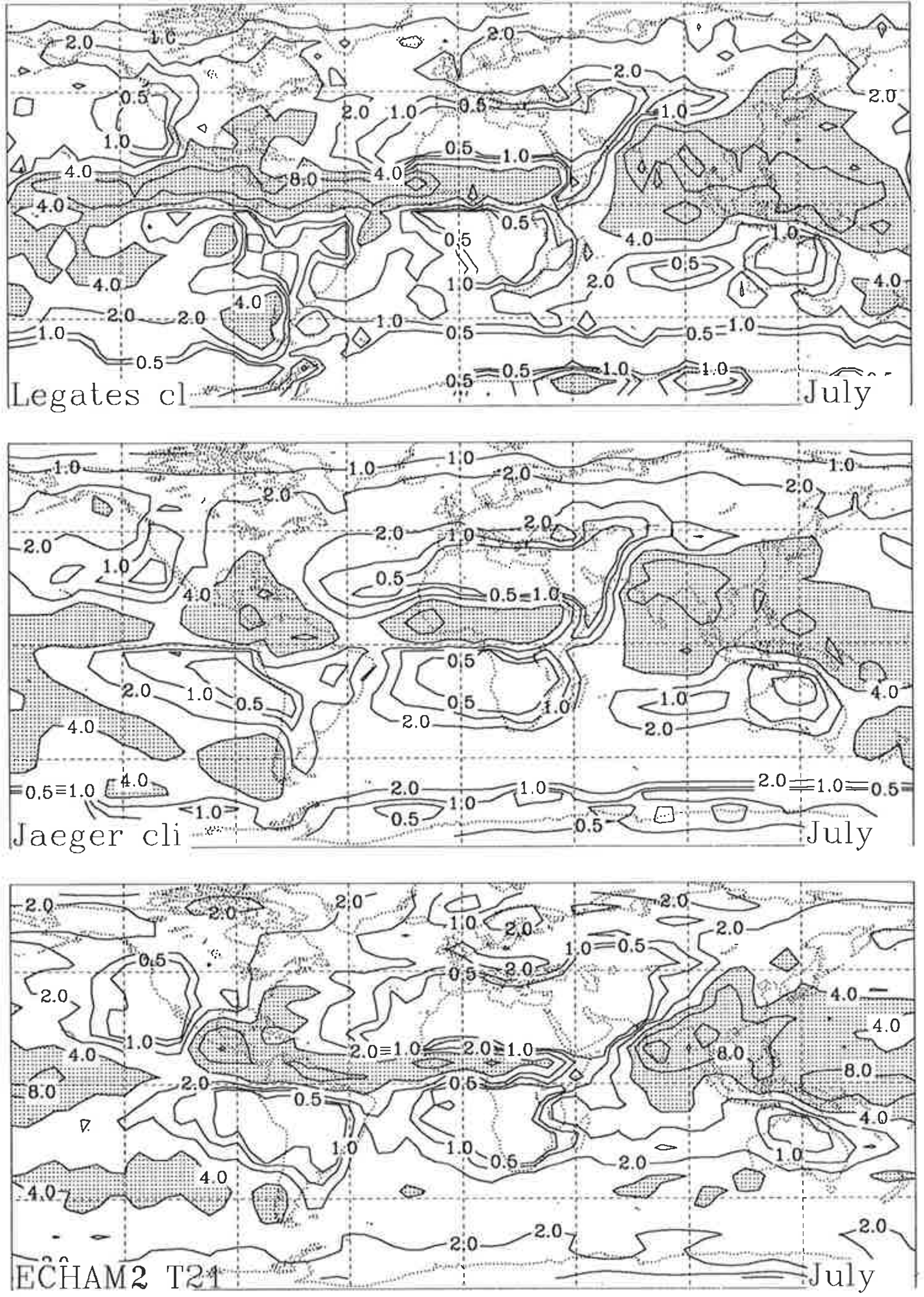

Fig. 7 (continued). b. As Figure 7a but for July.

In July, the larger-scale sinking motions that cause dryness over the subtropical continents, are well represented by the model in the Southern Hemisphere, but too far extended in the Northern Hemisphere. The ITCZ, although much more pronounced than in winter, does not extend far enough to the north. In some aspects the model ITCZ compares very well with Legates' (1987; Legates and Willmott, 1989) climatology. Also in the monsoon region the model simulated precipitation is in better agreement with this latter dataset (not shown).

4.2. Local runoff

The quantity of local runoff (Figure 8) at the surface is derived from the precipitation field according to the Arno scheme as described in section 3. The rainfall part of the precipitation is subjected to the scheme immediately and also drainage is computed at each time step. The amount of precipitation that falls as snow during the cold season is first stored in the snow pack until the melting season begins and is therefore subjected to the scheme with considerable delay.

We are at present not in a position to verify the time evolution of the local surface runoff for the continents in the OAGCM by direct comparison with observations. There is no information on how much runoff will occur at a certain grid cell for a given amount of precipitation. Even if this type of information were available, the Arno scheme would not stand up to a local verification, because of the current restriction on the variation of the parameter *b* as a function of orography only. So far no variation of land surface (soils) characteristics is applied. Considering this, we can only expect the simulated runoff field to represent — in a qualitative sense — the rainfall/runoff coefficients that mainly reflect mountainous regions and a consistent picture of the more trivial process of larger runoff in areas with higher amounts of rainfall and/or snow melt and soil water. Figure 8 shows that the scheme represents this very well, without an undue overestimation of the orography component.

During the annual cycle (Figure 8) we see that the model represents maximum runoff in the tropical regions, into which the Intertropical Convergence Zone migrates. In winter, Europe and the coastal areas of the North American continent, experience large runoff due to the high amounts of rainfall. Where the precipitation falls as snow, e.g. in Siberia, almost no runoff occurs during the winter months. It is not until April that large parts of the Northern Hemisphere continents experience high surface runoff as a result of the melting of the snow pack. The behaviour of the model snow pack was diagnosed to be in better agreement with observations in Eurasia than in North America (Behr and Dümenil, 1991). The snow cover there is deeper than observed and therefore more water is available for snow melt in the spring.

The change in the season from spring to summer is very marked in the tropics and the northern parts of the American and Eurasian continents. The ITCZ has now moved north of the equator, and on the Indian subcontinent and in South East Asia the monsoon has set in. Overall, the seasonal cycle of model generated local runoff seems to be acceptable. The global mean value of local runoff over the continents at 38 × 10^3 km/year is in good agreement with observations by Baumgartner and Reichel (1975).

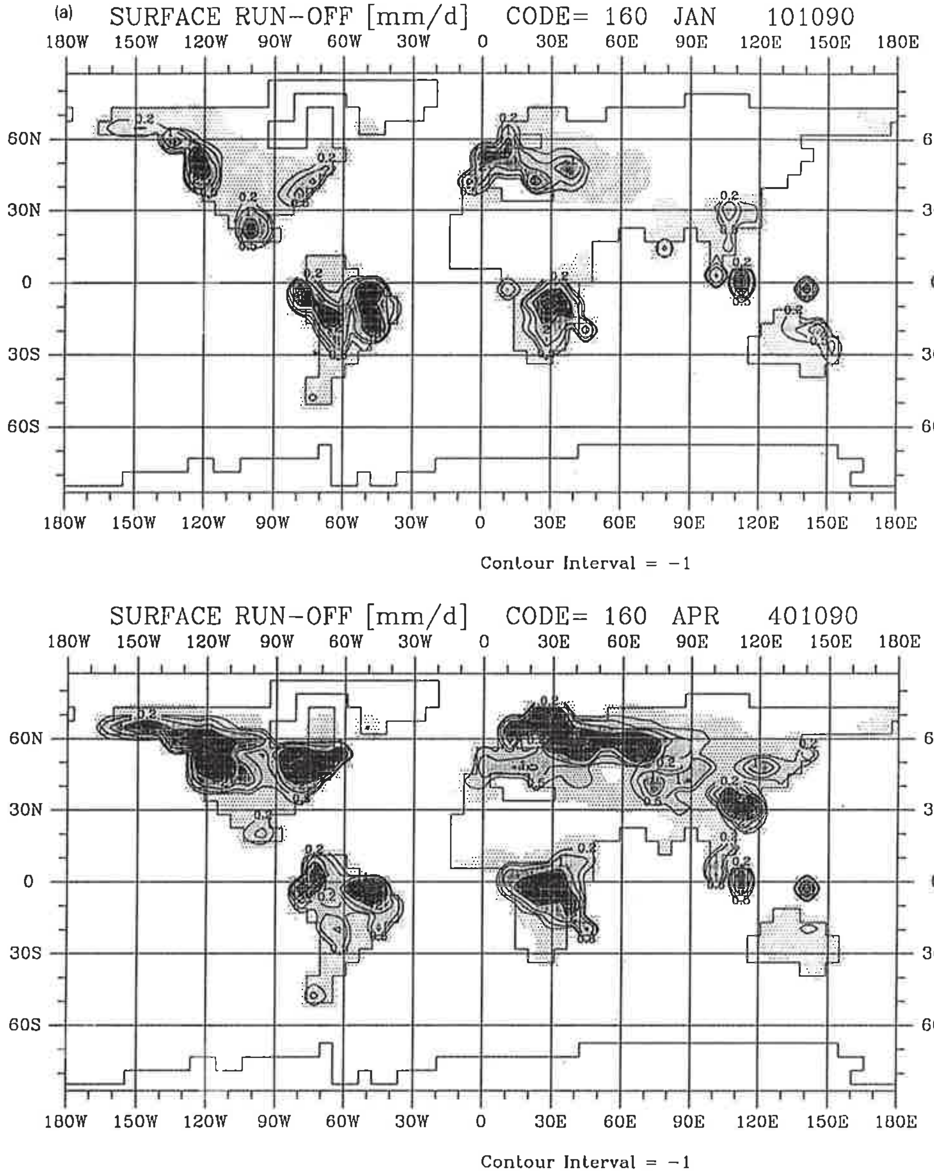

Fig. 8. a. Local surface runoff computed by the Arno model in the OAGCM. Values are from a 20-year integration with the ECHAM2 model for January (top) and April (bottom).

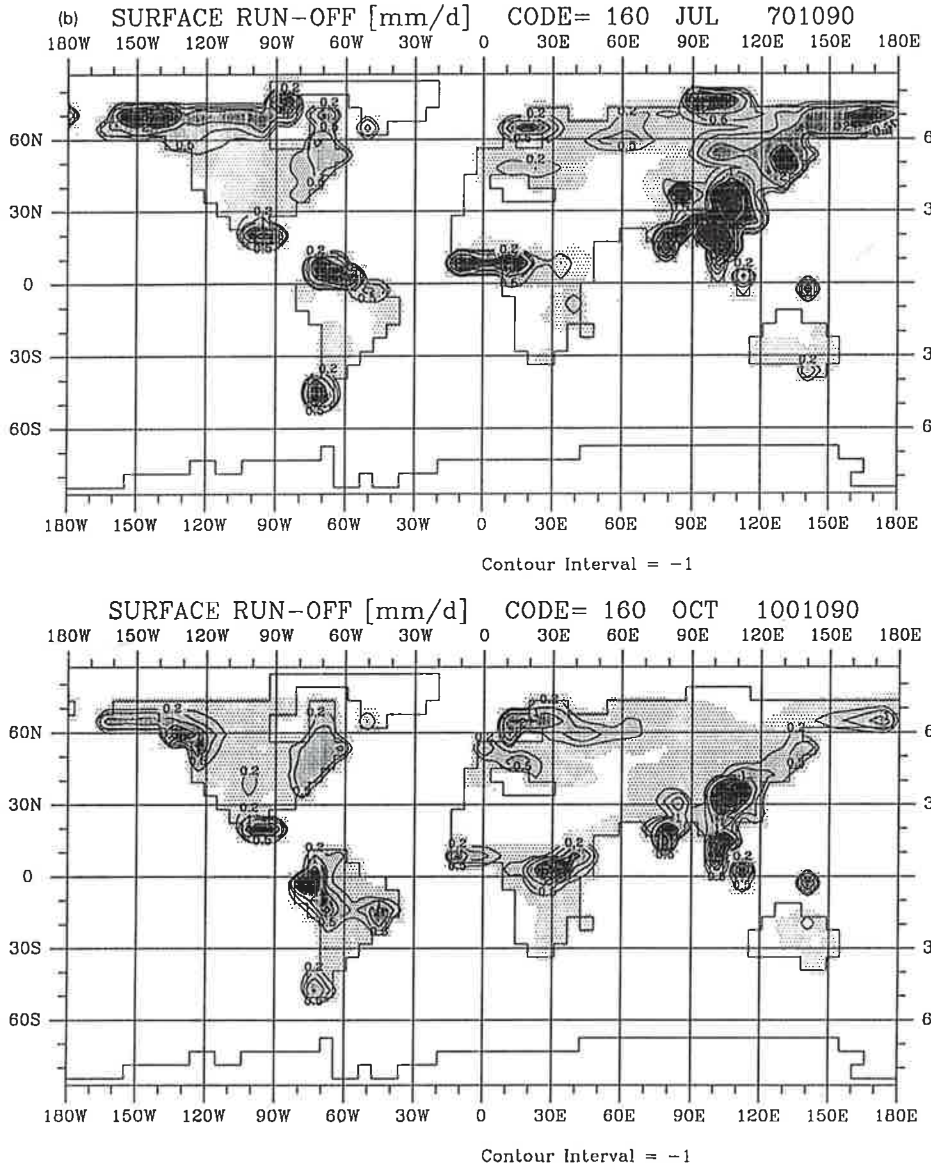

Fig. 8 (continued). b. Values for July (top) and October (bottom).

4.3. *Soil water*

The surface runoff is also steered indirectly by the amount of evaporation that occurs in a grid cell, because evaporation is a component of the soil water budget. An evaporation climatology has also been derived by Mintz and Serafini (1981) but it is not independent of the soil water climatology by the same authors. We shall therefore discuss only the latter. The performance of the soil water reservoir cannot yet be validated directly against observations on the OAGCM scale. Mintz and Serafini (1981) have derived a global field of large-scale "soil water" from observed precipitation and evaporation derived from a simple model. Figure 9 compares the results from the OAGCM with this surrogate climatology. In addition we now have to realize that systematic errors may be introduced by the atmospheric demand for water vapour (general circulation) and the formulation of the parameterisation scheme for evapotranspiration.

With a few exceptions, the model simulation of the general features of the seasonal cycle of soil wetness is in good agreement with the climatology. In the climatology we distinguish between the dry desert regions in the subtropics caused by descending air motion and the wet tropical areas where precipitation is abundant. In the model simulated field, the very dry regions are also well positioned in the subtropics (e.g. in July), but are less dry than in the climatology.

The largest differences with reference to the soil water reservoir occur in those regions, where the model simulates a melting snow pack. There are two reasons for this disagreement: first, the model snow pack is deeper than observed and the melting is delayed (as e.g. in North America), and, second, the climatology does not account for the process of snow melt. It was derived using precipitation data and an evapotranspiration model only (Serafini, pers. commun., 1990).

During the winter months, the South American continent is much drier in the model than in the climatology. This is due to a systematic model error in the precipitation field caused by the general circulation and is not sensitive to changes in the parameterisation of soil hydrology.

Soil wetness is also an OAGCM parameter that cannot be observed directly. For the purpose of OAGCM validation, surrogates are needed. If the local runoff in the model can be collected in large river catchments by a river routing or river runoff scheme (e.g. Sausen et al., 1991) the time delay between local runoff at a grid cell and river gauge measurements can be represented. We can then compare model results with river gauge data measured at the mouths of the largest rivers as an additional verification tool.

4.4. *River gauge data*

Validation of monthly mean values against river gauge data can provide a useful independent measure of model performance. It may complement the data from climatologies which are, at present, insufficient and unreliable. This type of data is being collected in a global data base and an effort is being made to create a comprehensive climatological dataset for the purpose of OAGCM validation for the twenty largest rivers in the world (Global Runoff Data Centre, Koblenz, F.R.G.). Until an agreed dataset (corrected for irrigation, sufficiently long time series, etc.) becomes available, validation studies can only be considered as preliminary attempts.

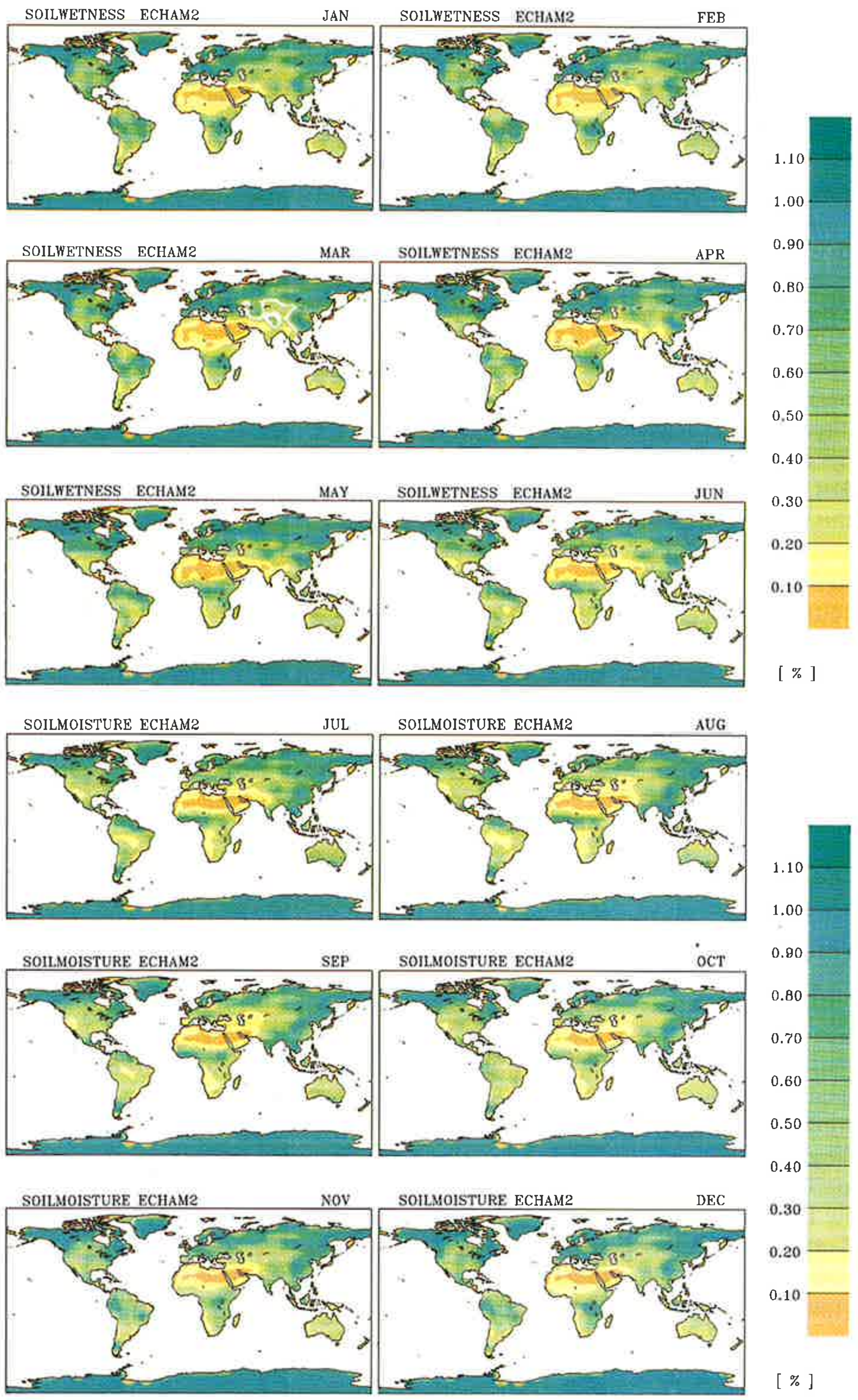

Fig. 9. Soil wetness as computed by the ECHAM2 model during the annual cycle.

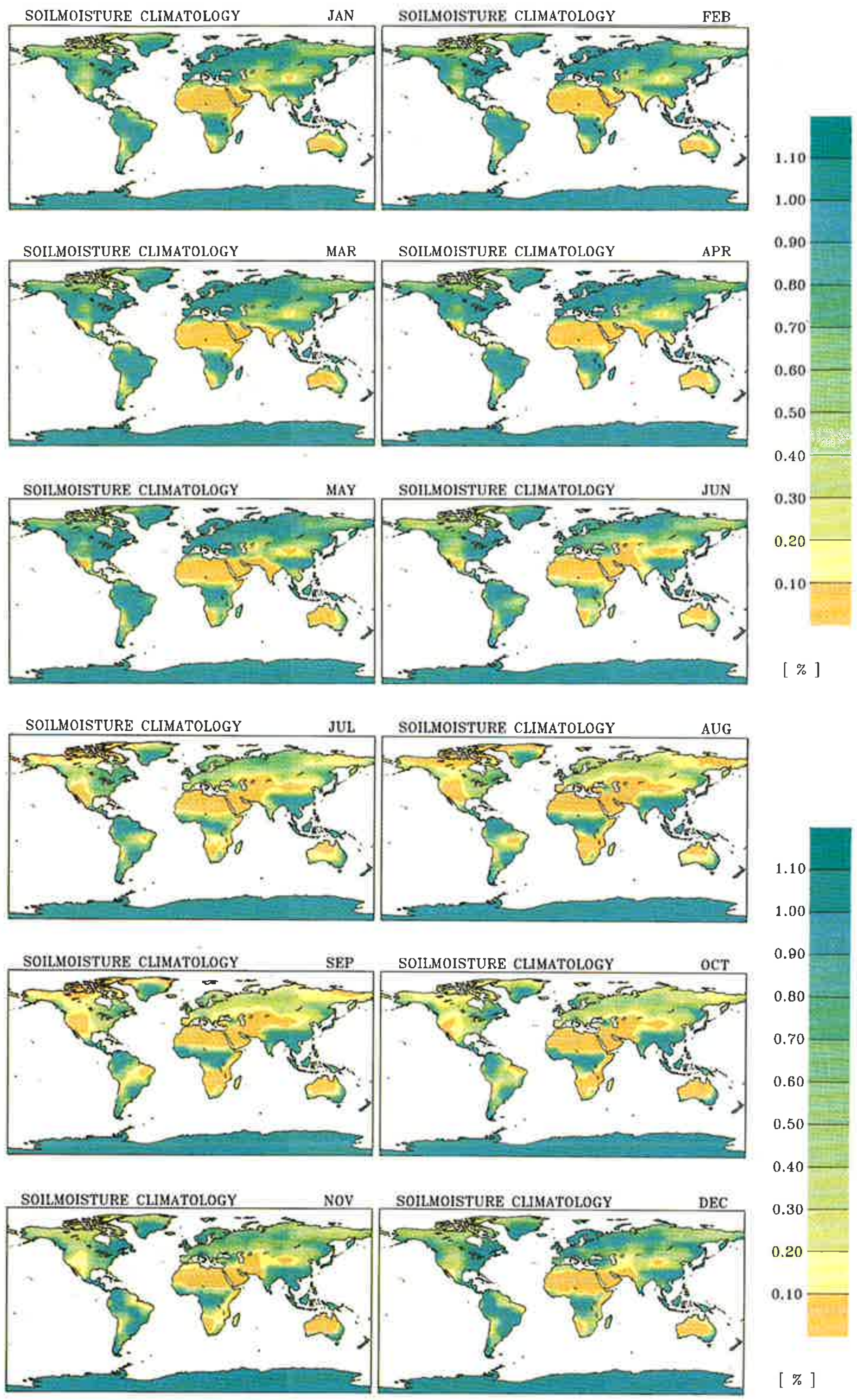

Fig. 9 (continued). Climatology is redrawn from Mintz and Serafini (1981).

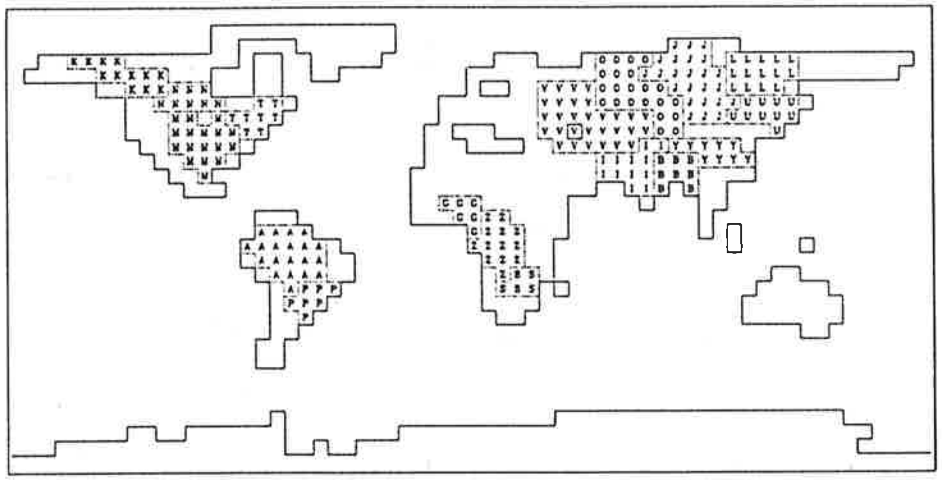

Fig. 10. Catchments of the largest rivers which are consistent with the ECHAM2-T21 model and its orography from Sausen et al. (1991).

Figure 10 shows the catchments which are consistent with the ECHAM2 model configuration. They may not always agree with the real catchments. Figure 11 shows the simulated and observed annual cycles of water, reaching the mouths of several large rivers. Considering only this small selection of rivers with large catchments we find that the model results vary between very good agreement (Lena, Jenissei) and total disagreement (Niger, St. Lawrence). There is a considerable variation in the observed maxima which have only been averaged in a crude way for this study and are not corrected for irrigation, etc.

Most of the deficiencies are, however, explained by the systematic model errors in the precipitation field. For example, the large amount of water transported by the Amazon river is also well represented by the model, but during the second half of the annual cycle, the model produces less rainfall than observed, so that the runoff is reduced almost to zero.

The fact that the Asian Monsoon season is well represented by the ECHAM2 model is reflected in the good agreement found for the Indus river and the Brahmaputra/Ganges.

The strong disagreement seen for the Niger river in Africa will require further investigation. It is likely that irrigation is the cause of the bias in the observed data available to us. The main part of the difference is, however, due to the bad representation of rainfall in the model's ITCZ in winter.

In general, the rivers dominated by snow melt in the spring are in good agreement with observations in Eurasia. We have already remarked that the model's deeper snow pack in North America disappears later in the year, than observed from other independent sources using snow data (Behr and Dümenil, 1991). Hence the disagreement with the river gauge data in the spring in this case is not surprising. In Eurasia where the simulated snow values agree much better with observations,

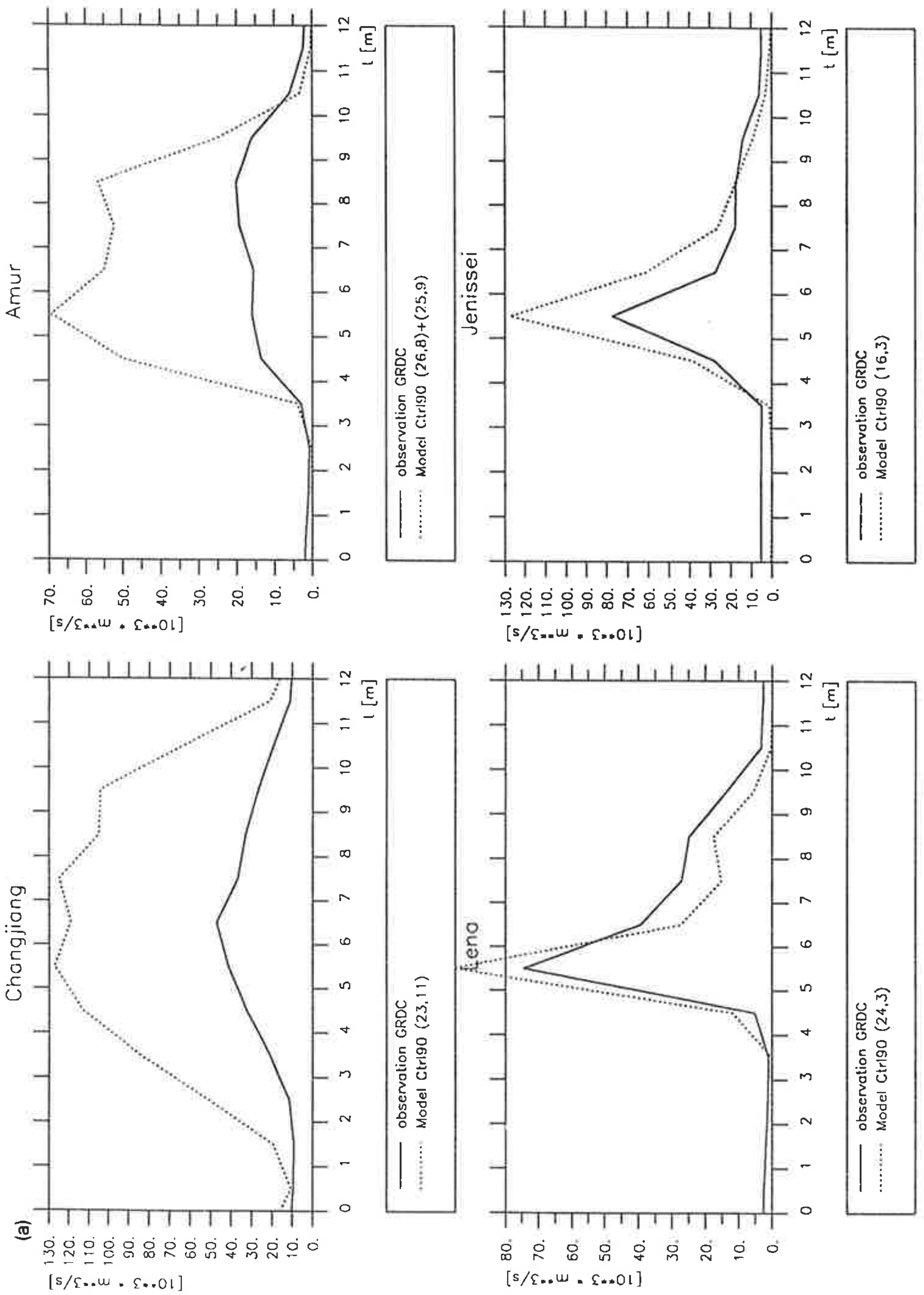

Fig. 11. Results from the 20-year integration with the ECHAM2-T21 model to which the river-runoff scheme by Sausen et al. (1991) was applied. Observations (full lines) are multi-year monthly averages which were kindly provided by GRDC, Koblenz, F.R.G. Model results are 20-year average discharges at the model grid points representative for the river (in brackets).

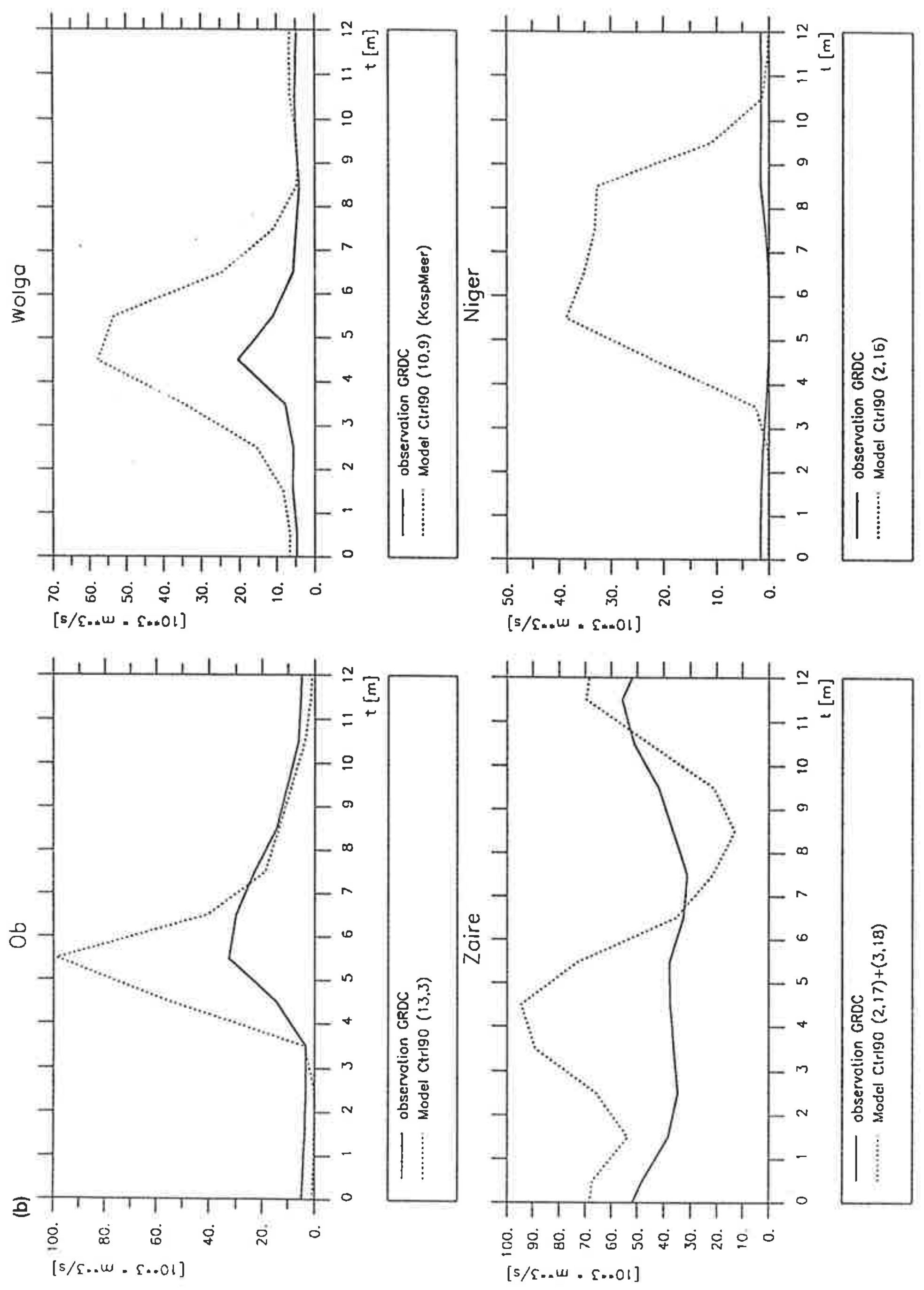

Fig. 11 (continued).

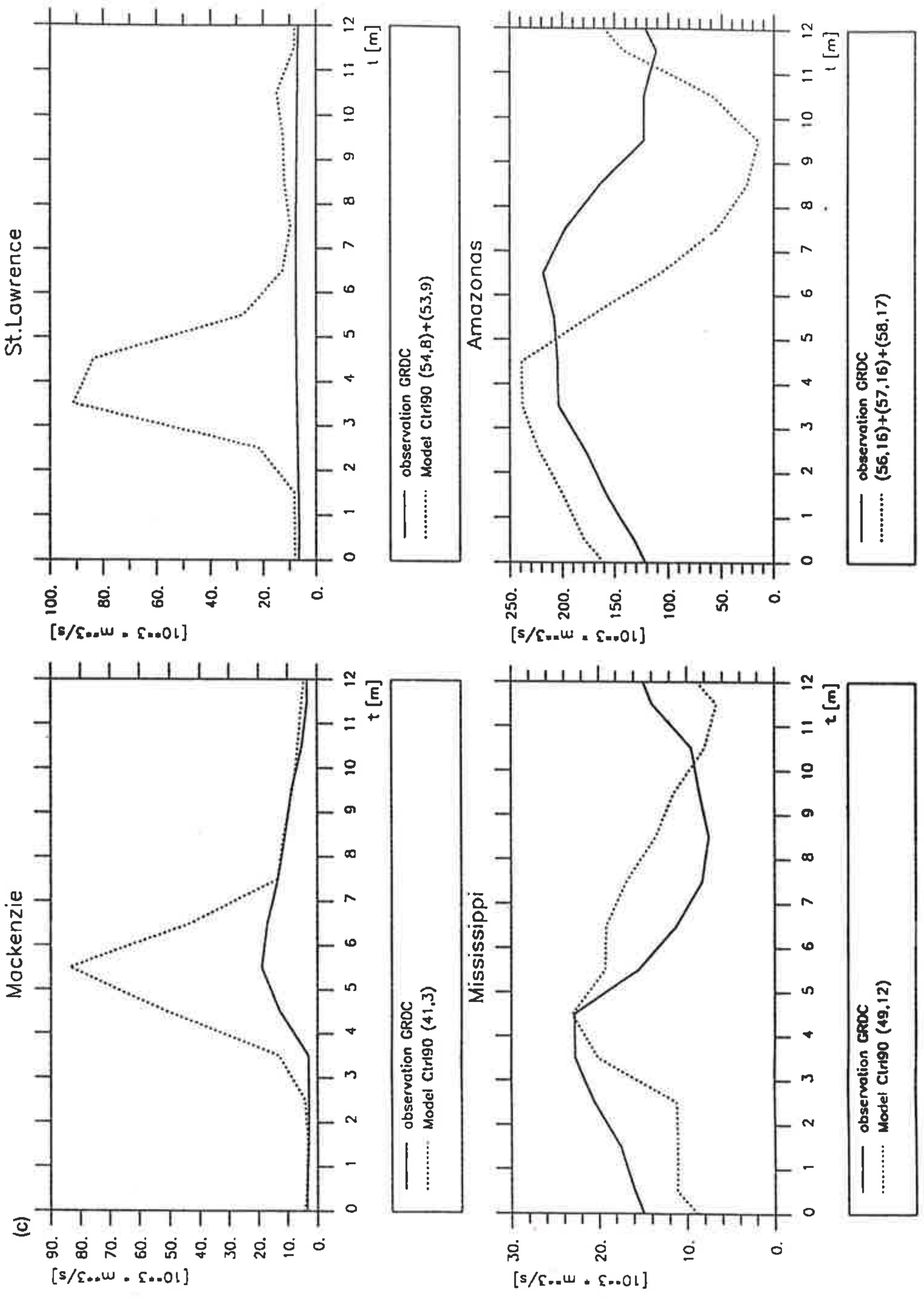

Fig. 11 (continued).

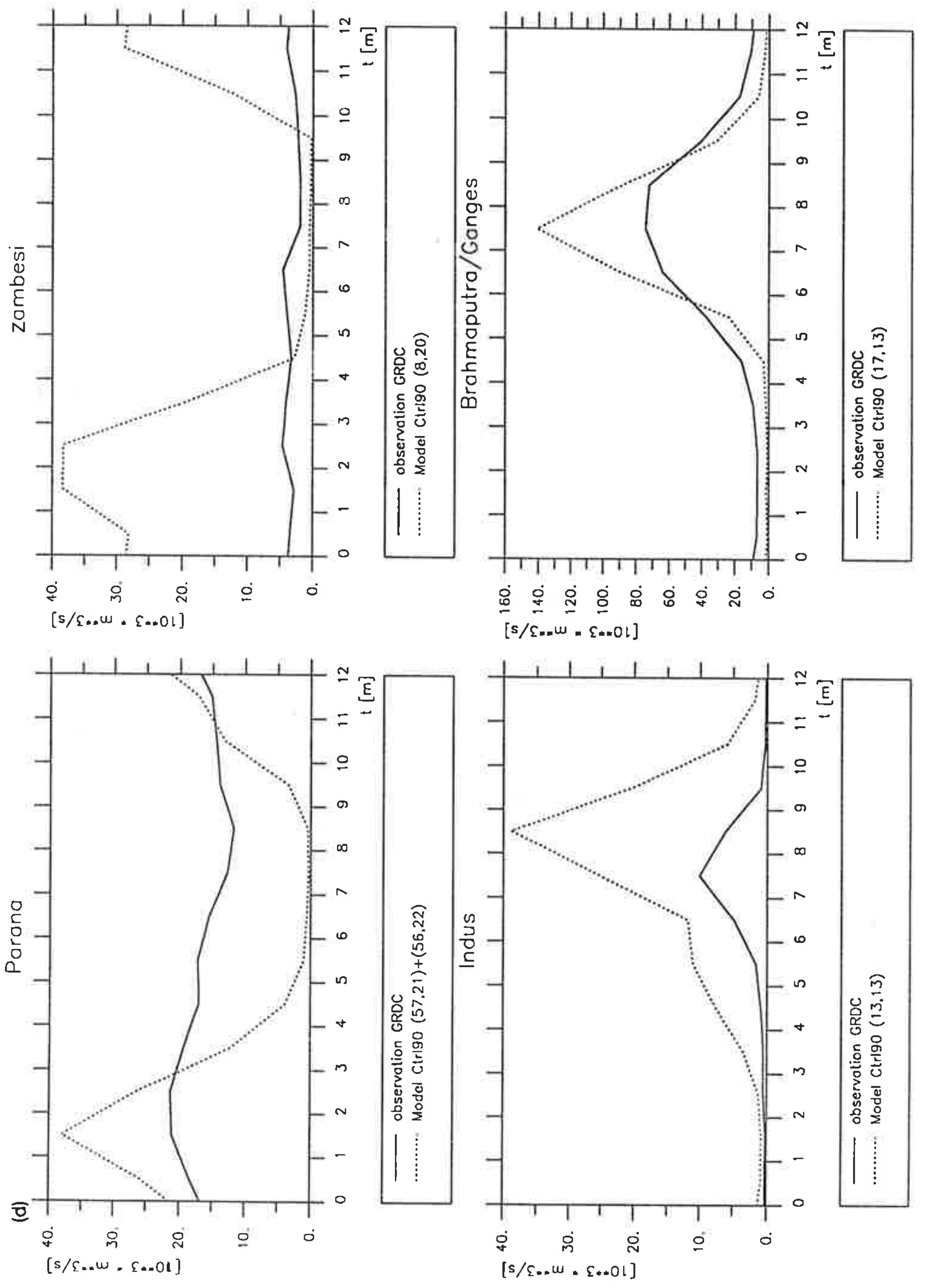

Fig. 11 (continued).

the model simulation, as a consequence, is in much better agreement with observed river gauge data.

5. Conclusions

The use of coupled ocean–atmosphere general circulation models for climate modelling, requires the computation of the time evolution of rainfall/runoff over the continents, which is one of the coupling parameters. The representation of this quantity in the OAGCM relies on two parameterisations: first, the specification of local runoff at a grid cell during a precipitation event and from the slowly acting drainage in the soil; second, the local runoff is collected in large river catchments and transferred to the river mouths, where it enters the ocean as freshwater input.

In the present paper we have discussed how the hydrological scheme for rainfall/runoff which was developed for the prediction of the water level of the river Arno, fulfils the requirements of the OAGCM. The heterogeneity of the land surface conditions over a grid area, determines the separation of rainfall between infiltration into the soil and surface runoff.

The scheme therefore is a first attempt at aggregating the physical processes at the point scale to the large scale of the OAGCM.

Applied in a 20-year integration with the ECHAM2 OAGCM, the scheme allows a consistent description of the various components of the hydrological cycle in the tropics, as well as, in the snow-covered regions of the Northern Hemisphere continents. We have attempted to validate qualitatively the model simulated hydrological cycle using independent sources of meteorological and hydrological data. In the future, gauge data from the largest rivers of the world will provide a particularly useful tool for independent verification of model results.

In its present configuration, the scheme is restricted to a uniform distribution of the precipitation over the grid cell. Future work will be directed at incorporating the small-scale features of the distribution of precipitation in space and time. It will also be necessary to expand the scheme, which is now restricted to one simple soil type, to soil types that vary for each grid cell. This should allow for a larger variability of the local runoff on the continental scale. At each grid point, the parameter b would then have to be computed as a function of soil type as well as orography.

The verification data and data for the initialisation of such extended schemes will have to be provided by the global experimentation and data collection exercises planned for the next decade.

Acknowledgement

Part of this work was carried out under the European Community Research Programme on Climatology, EPOCH project EV4C 0025I on Spatial Variability of Land Surface Processes.

References

Abbott, M. et al., 1986. An introduction to the European Hydrological System — Système Hydrologique Européen, SHE; 1. History and philosophy of a physically based distributed modelling system. J. Hydrol., 87: 45–59.

Baumgartner, A. and Reichel, E., 1975. The World Water Balance: Mean Annual Global Continental and Maritime Precipitation, Evaporation and Runoff. R. Oldenbourg, München–Wien.

Behr, H. and Dümenil, L., 1991. The snow climatology in decadal model simulations. Large-Scale Modelling Report No. 9, Meteorologisches Institut der Universität Hamburg, Hamburg, F.R.G.

Blondin, C., 1989. Research on land-surface parameterisation schemes at ECMWF. Proc. Workshop on Parameterisation of Fluxes over Land Surface, 24–26 October 1988, ECMWF, Reading, U.K.

Burnash, R.J.C., Ferral R.L. and McGuire, R.A., 1973. A general streamflow simulation system — conceptual modelling for digital computers. Report by the Joint Federal State River Forcasts Center, Sacramento, Calif.

Crawford, N.H. and Linsley, R.K., 1966. Digital simulation in hydrology, Stanford Watershed model IV. Tech. Rep. 39, Dep. Civil Eng. Stanford Univ., Stanford, Calif.

Deardorff, J.W., 1972. Parameterization of the planetary boundary layer for use in general circulation models. Mon. Weather Rev., 100: 93–106.

Fischer, G. (Editor), 1987. Climate simulations with the ECMWF T21 model in Hamburg. Large-Scale Atmospheric Modelling Report No. 1, Meteorologisches Institut der Universität Hamburg, Hamburg, F.R.G.

Jaeger, L., 1976. Monatskarten des Niederschlags für die ganze Erde. Berichte des Deutschen Wetterdienstes Nr. 139, Bd. 18, Offenbach/Main.

Legates, D.R., 1987. A climatology of global precipitation. Publ. Climatol. 40(1), Newark, Del., 85 pp.

Legates, D.R. and Willmott, C.J., 1990. Mean seasonal and spatial variability in gauge-corrected global precipitation. Int. J. Climatol., 10: 111–127.

Manabe, S., 1969. Climate and ocean circulation: I. The atmospheric circulation and the hydology of the earth's surface. Mon. Weather Rev., 97: 739–774.

Mintz, Y. and Serafini, V., 1981. Global field of soil water and land surface evapotranspiration. NASA Goddard Flight Center Tech. Memo. 83907, Res. Rev. 1980–1981, pp. 178–180.

Rocwood, D.M. and Nelson, M.L., 1966. Computer application to streamflow synthesis and reservoir regulation, IV Int. Conf. on Irrigation and Drainage.

Roeckner, E., Dümenil, L., Kirk, E., Lunkeit, F., Ponater, M., Rockel, B., Sausen R. and Schlese, U., 1989. The Hamburg version of the ECMWF model. In: G.J. Boer (Editor), Research Activities in Atmospheric and Oceanic Modelling. CAS/JSC Working Group on Numerical Experimentation, 13, WMO/TD-No. 332, pp. 7.1–7.4.

Roeckner, E., Arpe, K., Bengtsson, L., Brinkop, S., Dümenil, L., Kirk, E., Lunkeit, F., Esch, M., Ponater, M., Rockel, B., Sausen, R., Schlese, U., Schubert, S. and Windelband, M., 1992. Simulation of the present-day climate with the ECHAM model: impact of model physics and resolution. Max Planck Institute Report No. 95.

Sausen, R., Schubert S. and Dümenil, L., 1991. A model of the river-runoff for use in coupled atmosphere–ocean models. Large-Scale Atmospheric Modelling Report No. 9, Meteorologisches Institut der Universität Hamburg, Hamburg, F.R.G.

Sittner, W.T., Schaus C.E. and Monro, J.C., 1969. Continuous hydrograph synthesis with an API-type hydrologic model. Water Resour. Res., 5(5): 1007–1022.

Sugawara, M., Ozaki, E., Watanabe, I. and Katsuyama, Y., 1976. Tank Model and its application to Bird Creek, Wollombi Brook, Bihin River, Sanaga River, and Nam Mune. Research Notes of the National Centre for Disaster Prevention, No. 11, Tokyo.

Todini, E., 1988. Il modello afflussi deflussi del fiume Arno. Relazione Generale dello studio per conto della Regione Toscana, University of Bologna.

Warrilow, D.A., Sangster A.B. and Slingo, A., 1986. Modelling of land surface processes and their influence on European climate. DCTN 38, U.K. Meteorological Office, Bracknell, U.K.

Zhao, R.J., 1977. Flood forecasting method for humid regions of China. East China College of Hydraulic Engineering, Nanjing, China.